



Title	A generic tight-binding model for monolayer, bilayer and bulk MoS₂
Author(s)	Zahid, F; Liu, L; Zhu, Y; Wang, J; Guo, H
Citation	AIP Advances, 2013, v. 3, p. 052111
Issued Date	2013
URL	http://hdl.handle.net/10722/186159
Rights	Creative Commons: Attribution 3.0 Hong Kong License

A generic tight-binding model for monolayer, bilayer and bulk MoS₂

Ferdows Zahid,^{1,a} Lei Liu,² Yu Zhu,² Jian Wang,¹ and Hong Guo³

¹Department of Physics, The University of Hong Kong, Pok Fulam Road, Hong Kong SAR, China

²Nanoacademic Technologies Inc., Brossard, Quebec, J4Z 1A7, Canada

³Centre for the Physics of Materials and Department of Physics, McGill University, Montreal, PQ, H3A 2T8, Canada

(Received 28 March 2013; accepted 29 April 2013; published online 8 May 2013)

Molybdenum disulfide (MoS₂) is a layered semiconductor which has become very important recently as an emerging electronic device material. Being an intrinsic semiconductor the two-dimensional MoS₂ has major advantages as the channel material in field-effect transistors. In this work we determine the electronic structures of MoS₂ with the highly accurate screened hybrid functional within the density functional theory (DFT) including the spin-orbit coupling. Using the DFT electronic structures as target, we have developed a single generic tight-binding (TB) model that accurately produces the electronic structures for three different forms of MoS₂ - bulk, bilayer and monolayer. Our TB model is based on the Slater-Koster method with non-orthogonal sp³d⁵ orbitals, nearest-neighbor interactions and spin-orbit coupling. The TB model is useful for atomistic modeling of quantum transport in MoS₂ based electronic devices. © 2013 Author(s). All article content, except where otherwise noted, is licensed under a Creative Commons Attribution 3.0 Unported License. [<http://dx.doi.org/10.1063/1.4804936>]

Molybdenum disulfide (MoS₂) belongs to a family of layered transition metal dichalcogenides (TMDC) in which the layers are held together by weak van der Waals forces, and it can be exfoliated mechanically to a single layer thickness. In its bulk form MoS₂ is an indirect band gap semiconductor which turns into a direct band gap semiconductor for monolayer structure.¹ This intrinsic semiconducting nature of MoS₂ is a major advantage over graphene (which has no intrinsic band gap) as a two-dimensional (2D) channel material in field-effect transistors (FET). Indeed, FET devices based on MoS₂ monolayer and bilayer have already been fabricated in the experimental labs and demonstrated to have useful device performances.^{2,3} Several theoretical studies of MoS₂ FET devices⁴⁻⁶ based on simplified description of the electronic structures within an effective mass model have also been reported recently.

Due to the complex nature of the layered TMDC materials and the great interests in the electronics community for its applications in emerging devices, a more reliable, accurate, and atomistic treatment of the electronic structures of TMDC is desired. Since *ab initio* models are computationally expensive and often intractable for realistic device structures having large number of atoms, a widely applied intermediary option is the tight-binding (TB) model. TB models are atomistic full-band yet computationally efficient due to the small number of basis orbitals and the rigid nature of the Hamiltonian. Properly parameterized TB models have been extensively applied to predict reliable results for a diverse range of devices including the resonant tunneling diodes,⁷ quantum dots,⁸ Si nanowireFET,⁹ and compound semiconductor heterostructures.¹⁰

In this study, we report a *generic* TB model with non-orthogonal sp³d⁵ orbitals including the nearest-neighbour interactions and spin-orbit coupling, that accurately determines the electronic

^aElectronic mail: fzahid@hku.hk



structures of bulk, monolayer and bilayer MoS₂. A reliable and accurate target band structure is the primary requirement for a successful tight-binding modeling. For the calculations of the target band structures we employ density functional theory (DFT) with the screened hybrid functional of Heyd, Scuseria, and Ernzerhof¹¹ (HSE) that has been shown in the literature^{12–14} to produce accurate band gaps and reasonable effective masses for a wide range of semiconductors. Our calculated band structures of MoS₂ from the self-consistent DFT-HSE shows excellent agreement with the available experimental data and compare well with other theoretical studies.^{15–17} Even though an accurate target band structure is obtained by DFT-HSE, it is nontrivial to develop a *generic* TB model which can accurately capture electronic structures and effective masses of not only bulk MoS₂ but also its double-layer and single-layer forms. For the layered TMDC structures there is a thickness dependent interlayer interaction that significantly affects the electronic properties, the TB model must capture these effects so as to be applicable to devices made of different layer thicknesses. As shown below, our *generic* TB model accurately produces the band structures for three different forms of MoS₂: bulk, monolayer and bilayer. The reported TB model can be easily extended to other MoS₂ structures of higher number of layers as well as other layered TMDC materials such as WS₂, WSe₂, and MoSe₂. The accuracy of our TB model is validated by comparing the band gaps and effective masses with our calculated *ab initio* results.

In our study, all the DFT-HSE calculations are performed using the projector augmented-wave (PAW) pseudopotential plane-wave method as implemented in the VASP software package.¹⁸ A Monkhorst-Pack scheme is adopted for the sampling of the Brillouin zone with k-point meshes of $7 \times 7 \times 2$ for the bulk and $9 \times 9 \times 1$ for the two-dimensional (2D) structures. An energy cutoff of 280 eV is used in a plane wave basis set. We also included the spin-orbit coupling self-consistently. Due to the presence of van der Waals interaction which determines the interlayer distance in MoS₂, geometry optimization becomes quite tricky and complicated. Without the van der Waals interaction the lattice parameter c (vertical length of the unit cell) is overestimated by a large margin. However, it is not yet possible to include van der Waals interaction in the HSE calculations, and it is an area of active research. We therefore optimize the bulk crystal structure using the Perdew-Burke-Ernzerhof (PBE) functional¹⁹ for which the van der Waals interaction can be included explicitly by adopting the DFT-D2 method.²⁰ We then use this optimized structure for the HSE calculations. The values of our optimized lattice parameters for bulk MoS₂ are: $a = 3.179 \text{ \AA}$ and $c = 12.729 \text{ \AA}$ with a layer thickness of 3.135 \AA (S-S vertical distance). Although the value of c parameter improves significantly with the DFT-D2 method, it is still overestimated by around 3.6% compared to the experimental value.

It is a well-known fact that DFT within the local density approximation (LDA) or the generalized gradient approximation (GGA) underestimates band gaps of semiconductors due to factors such as the self interactions. This error can be minimized in the HSE scheme of hybrid functional method¹¹ by incorporating 25% short-range (SR) exact Hartree-Fock (HF) exchange with the PBE functional. A screening parameter μ defines the range separation, and is empirically set to 0.2 \AA^{-1} (HSE06 scheme) for both the HF and PBE parts. In our calculations for MoS₂ we observe that the band gap energies vary significantly with the screening parameter for both the bulk and the 2D structures. We therefore decided to adjust the value of μ to fit the experimental band gap, and an optimized value for μ is found to be 0.4 \AA^{-1} which corresponds to an interaction range of $\pi/\mu = 7.85 \text{ \AA}$ for the SR nonlocal exchange. Note that a single value of μ is used for all the three structures of MoS₂: bulk, double-layer and single-layer, namely the HSE results presented here were all obtained using $\mu = 0.4 \text{ \AA}^{-1}$.

Our calculated band structure results for MoS₂ are plotted in Fig. 1. As observed in previous studies^{15,16,21} we also notice from our DFT-HSE calculations that the monolayer MoS₂ has a direct band gap at the K point whereas an indirect band gap opens up due to the presence of interlayer interactions in the bilayer and the bulk structures. Although both bulk and bilayer MoS₂ have indirect band gaps the conduction band minima (CBM) are located at different points: for bulk it is at Σ point (midpoint of Γ and K points) and for bilayer it is at K point. Similar behavior is observed in a previous theoretical study.¹⁵ For monolayer MoS₂ the splitting of the valence band maximum (VBM) at K point is solely due to the spin-orbit coupling (SOC) whereas a combination of SOC and interlayer interactions is responsible for the VBM splitting in bulk and bilayer MoS₂. With the self-consistent calculations of the spin-orbit effects within the DFT-HSE model we obtain a

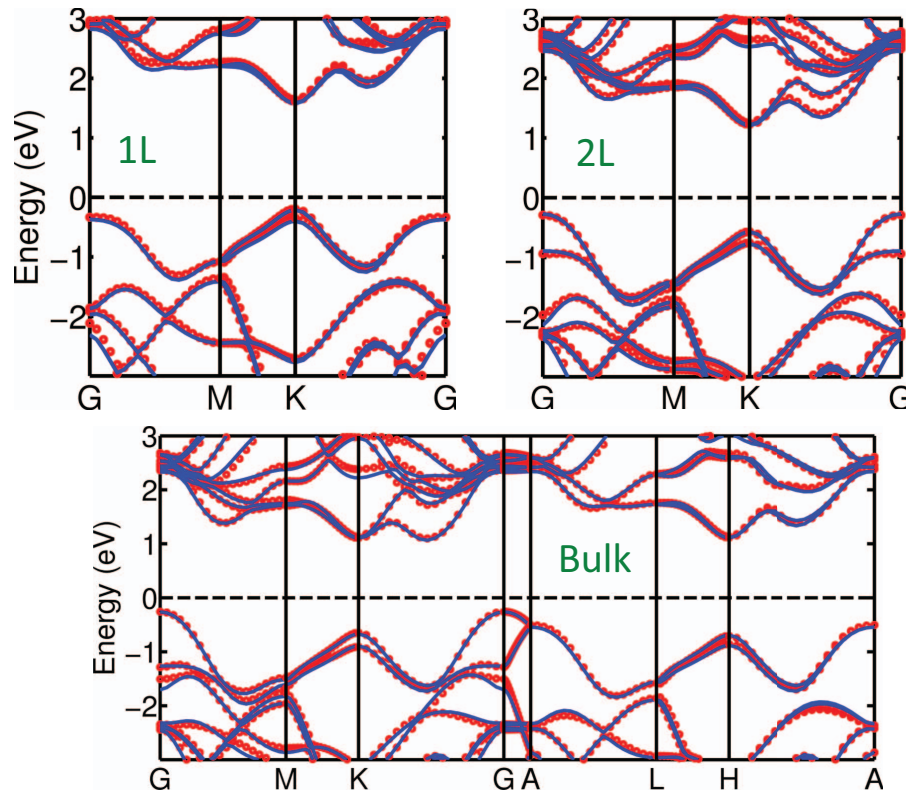


FIG. 1. Band structures for monolayer (1L), bilayer (2L), and bulk MoS₂ using screened hybrid density functional theory (blue lines) and our tight-binding fitting (red dots). The zero in the energy axis is set at the Fermi level as shown by the dashed line. Spin-orbit coupling is included in the calculations self-consistently.

TABLE I. Band gap energies obtained by DFT-HSE and our TB model. The fifth column is the deviation between the HSE and the TB values. Experimental data is shown in the sixth column, taken from Ref. 22 (for bulk) and Ref. 1 (for monolayer and bilayer). All the energies are in the unit of eV. Subscripts *v* and *c* stand for valence band and conduction band, respectively. The splitting of the valence band maximum at K point is given by K_{v1} (top) and K_{v2} (bottom), whereas Σ is the midpoint of the line joining the Γ and the K points.

Structure	Gap	HSE (target)	TB (fitted)	Deviation (%)	Exp.
Monolayer	K _{v1} to K _c	1.786	1.805	1.06	1.90
	K _{v2} to K _c	1.974	1.969	0.24	2.05
Bilayer	Γ _v to K _c	1.480	1.516	2.41	1.60
	K _{v1} to K _c	1.779	1.792	0.76	1.88
Bulk	K _{v2} to K _c	1.980	1.987	0.35	2.05
	Γ _v to Σ _c	1.328	1.331	0.22	1.29
	K _{v1} to K _c	1.776	1.749	1.46	1.88
	K _{v2} to K _c	1.960	2.009	2.46	2.06

split-off value of 188 meV for the VBM at K point for monolayer MoS₂, which is comparable to the experimental value of 150 meV. The splitting of CBM due to SOC is minimal (around 5 meV). The calculated band gap energies for different transitions are presented in Table I. Our DFT-HSE results show good agreement with the experimental data. The values of effective masses at different band edges along different directions as presented in Table II also compare well with other available theoretical studies.^{15,17}

With the calculated DFT-HSE band structures as target, we employed the Nanoskif²³ software package to obtain a set of TB parameters for the on-site energies, the Slater-Koster energy integrals,

TABLE II. Values of effective masses at various band edges in the unit of free electron mass (m_0) calculated using the HSE method and our tight-binding model. The subscripts l and t refer to the masses calculated at the point along the longitudinal and the transversal directions of the line connecting the Γ point and that point, respectively.

Structure	Point	Electron			Hole		
		HSE (target)	TB (fitted)	Deviation (%)	HSE (target)	TB (fitted)	Deviation (%)
Monolayer	K_l	0.407	0.430	4.58	0.485	0.463	4.54
	K_t	0.404	0.426	5.45	0.480	0.458	4.58
Bilayer	Γ				1.039	1.321	27.91
	K_l	0.430	0.457	6.28			
Bulk	K_t	0.423	0.454	7.33			
	Γ				0.785	0.917	16.82
	Σ_l	0.574	0.712	24.04			
	Σ_t	0.819	0.999	21.98			

TABLE III. Tight-binding parameters for MoS₂ using non-orthogonal model with sp^3d^5 orbitals, nearest-neighbour interactions, and spin-orbit coupling: on-site energies (E), spin-orbit splitting (λ), Slater-Koster energy integrals (E_1 for intra-layer and E_2 for inter-layer interaction) and overlap integrals (O_1 for intra-layer and O_2 for inter-layer interaction). The energies are in the unit of eV.

	E_s	E_p	E_d	λ_{SO}				
S	7.6595	-2.1537	8.7689	0.2129				
Mo	5.5994	6.7128	2.6429	1.0675				
	$E_1(S,Mo)$	$E_1(S,S)$	$E_2(S,S)$	$E_1(Mo,Mo)$	$O_1(S,Mo)$	$O_1(S,S)$	$O_2(S,S)$	$O_1(Mo,Mo)$
$ss\sigma$	-0.0917	0.3093	0.3207	0.1768	0.0294	-0.0532	-0.1430	-0.0575
$sp\sigma$	0.6656	-0.9210	-0.1302	1.0910	0.1042	0.0240	0.0196	0.0057
$ps\sigma$	-1.6515				0.1765			
$pp\sigma$	1.4008	0.7132	0.7053	-0.3842	-0.1865	0.0478	-0.0486	0.0296
$pp\pi$	-0.4812	-0.1920	-0.0980	0.5203	0.0303	-0.0104	0.0117	0.0946
$sd\sigma$	0.2177	-0.2016	0.1164	-0.5635	-0.0480	0.0946	0.0297	-0.1082
$ds\sigma$	-1.0654				-0.1432			
$pd\sigma$	-2.8732	-0.5204	-0.0334	-0.2316	0.0942	0.0724	-0.0087	0.0212
$dp\sigma$	2.1898				0.2002			
$pd\pi$	0.7739	-0.1203	-0.0370	0.0582	0.0132	0.0772	-0.0031	-0.0448
$dp\pi$	-1.9408				-0.2435			
$dd\sigma$	-3.1425	0.8347	-0.2300	0.3602	0.0273	0.1849	0.0060	-0.0216
$dd\pi$	2.4975	0.7434	0.0050	0.0432	0.1940	-0.0429	-0.0378	-0.0285
$dd\delta$	-0.3703	-0.1919	-0.1104	0.1008	0.1261	-0.0333	0.0007	0.0432

overlap integrals,²⁴ and the spin-orbit splitting.²⁵ In our TB model we adopted a non-orthogonal basis set of sp^3d^5 orbitals considering only the nearest neighbour interactions. The effects of spin-orbit coupling is included through a split-off energy term. A set of 96 parameters are optimized through the automated process built in Nanoskif.²³ The root-mean-square deviation of the fitting is within 25 meV. The optimized TB parameters are listed in Table III. Note that this single set of TB parameters is capable of producing accurate band structures of all three different forms of MoS₂.

The band structures obtained from our TB model are plotted in Fig. 1 along with those obtained from DFT-HSE. The agreement in energies around both VBM and CBM for all three structures of MoS₂ is excellent. Fig. 2 shows the energy contours around the valence band maximum (VBM) and the conduction band minimum (CBM) for the monolayer MoS₂. Again, we observe excellent agreement in the shape of the energy contours from DFT-HSE and TB fitting. The band gap energies for different transitions and the effective mass values at different symmetry points obtained from the DFT-HSE and the TB model are presented in Table I and Table II respectively. For the band gap energies a fitting accuracy of less than 2.5% is achieved. On the other hand, for the effective masses, in most cases the deviations between the DFT-HSE and the TB values are less than 10% which is

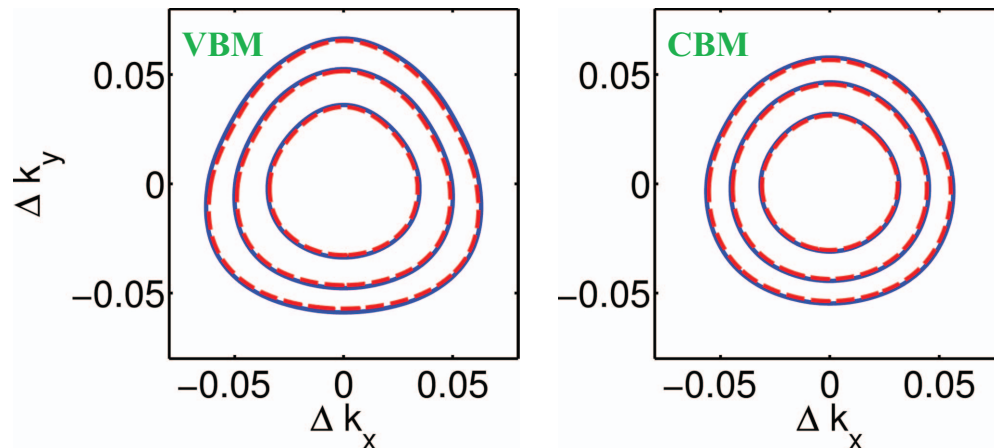


FIG. 2. Contour plots of the energies around the valence band maximum (VBM) and conduction band minimum (CBM) for monolayer MoS₂ from screened hybrid density functional theory (blue solid lines) and our tight-binding model (red dashed lines). The contour lines are associated with $\Delta E = \pm \frac{1}{30}, \pm \frac{1}{15}, \pm \frac{1}{10}$ eV, respectively and the Δk_x and the Δk_y are in the unit of $\frac{2\pi}{a}$, where a is the unit cell length.

quite acceptable. In four cases (excluding the monolayer structure) the deviations are higher with the worst situation at $\sim 27.9\%$. Given that just a single set of TB parameters is used to produce the band structures of all three different forms of the material, this level of quantitative consistency is rather satisfactory.

In conclusion, we have developed a generic TB model for accurately calculating the band structures of bulk, monolayer and bilayer MoS₂. Our TB model is based on the Slater-Koster method. For the optimization of the TB parameters, accurate target band structures are obtained using the screened hybrid DFT method. The accuracy of our TB model is verified by comparing the band gaps for different transitions and the effective masses at different band edges against the *ab initio* band structures. One main feature of our TB model is that with only one set of parameters it can reproduce the band structures of MoS₂ of different structural configurations: from bulk to 2D structures. Our tight-binding model can be easily extended to other TMDC materials that show electronic characteristics similar to MoS₂. The TB model reported in this paper is useful for simulations of quantum transport in nanoelectronic devices based on the TMDC materials.

ACKNOWLEDGMENTS

This work is supported by the University Grant Council (Contract No. AoE/P-04/08) of the Government of HKSAR (FZ, JW), NSERC (HG) and IRAP (LL, YZ) of Canada. F.Z. would like to thank Dr. Ji Wei and Mr. Darshana Wickramaratne for useful discussions on the VASP calculations.

- ¹ K. F. Mak, C. Lee, J. Hone, J. Shan, and T. F. Heinz, *Phys. Rev. Lett.* **105**, 136805 (2010).
- ² B. Radisavljevic, A. Radenovic, J. Brivio, V. Giacometti, and A. Kis, *Nat. Nanotechnol.* **6**, 147 (2011).
- ³ H. Liu and P. D. Ye, *IEEE Electron Dev. Lett.* **33**, 546 (2012).
- ⁴ Y. Yoon, K. Ganapathi, and S. Salahuddin, *Nano Lett.* **11**, 3768 (2011).
- ⁵ L. Liu, S. B. Kumar, Y. Ouyang, and J. Guo, *IEEE Trans. Electron Dev.* **58**, 3042 (2011).
- ⁶ K. Alam and R. K. Lake, *IEEE Trans. Electron Dev.* **59**, 3250 (2012).
- ⁷ R. C. Bowen, G. Klimeck, R. Lake, W. R. Frensley, and T. Moise, *J. Appl. Phys.* **81**, 3207 (1997).
- ⁸ M. Usman, H. Ryu, I. Woo, D. S. Ebert, and G. Klimeck, *IEEE Trans. Nanotechnol.* **8**, 330 (2009).
- ⁹ M. Luisier and G. Klimeck, *Phys. Rev. B* **80**, 155430 (2009).
- ¹⁰ U. E. Avci, S. Hasan, D. E. Nikonov, R. Rios, K. Kuhn, I. A. Young, *Symp. VLSI Tech.*, pp. 183 (2012).
- ¹¹ J. Heyd, G. E. Scuseria, and M. Ernzerhof, *J. Chem. Phys.* **118**, 8207 (2003); **124**, 219906 (2006).
- ¹² Y.-S. Kim, K. Hummer, and G. Kresse, *Phys. Rev. B* **80**, 035203 (2009).
- ¹³ Y.-S. Kim, M. Marsman, and G. Kresse, *Phys. Rev. B* **82**, 205212 (2010).
- ¹⁴ J. E. Peralta, J. Heyd, and G. E. Scuseria, *Phys. Rev. B* **74**, 073101 (2006).
- ¹⁵ T. Cheiwchanchamnangij and W. R. L. Lambrecht, *Phys. Rev. B* **85**, 205302 (2012).

- ¹⁶J. K. Ellis, M. J. Lucero, and G. E. Scuseria, *Appl. Phys. Lett.* **99**, 261908 (2011).
- ¹⁷H. Peelaers and C. G. Van de Walle, *Phys. Rev. B* **86**, 241401(R) (2012).
- ¹⁸G. Kresse, and J. Hafner, *Phys. Rev. B* **47**, R558 (1993); G. Kresse and J. Furthmuller, *ibid.* **54**, 11169 (1996).
- ¹⁹J. P. Perdew, K. Burke, and M. Ernzerhof, *Phys. Rev. Lett.* **77**, 3865 (1996).
- ²⁰T. Bucko, J. Hafner, S. Lebegue, and J. G. Angya, *J. Phys. Chem. A* **114**, 11814 (2010).
- ²¹E. S. Kadantsev and P. Hawrylak, *Solid State Commun.* **152**, 909 (2012); S. Lebegue and O. Eriksson, *Phys. Rev. B* **79**, 115409 (2009); Z. Y. Zhu, Y. C. Cheng, and U. Schwingenschlogl, *ibid.* **84**, 153402 (2011).
- ²²A. R. Beal and H. P. Hughes, *J. Phys. C* **12**, 881 (1979).
- ²³Nanoskif is a special tool developed by NanoAcademic Technologies Inc. (www.nanoacademic.com) for the optimization of the Slater-Koster energies and/or overlap integrals used in the tight-binding models by fitting a target band structure of a system, or a set of band structures of several systems simultaneously, employing state-of-the-art algorithms.
- ²⁴J. C. Slater and G. F. Koster, *Phys. Rev.* **94**, 1498 (1954).
- ²⁵D. J. Chadi, *Phys. Rev. B* **16**, 790 (1977).